Journal of Computational Science and Technology

Vol. 3, No. 1, 2009

Simple Modelling and Strength Evaluation Methods for Bolt Joints Using Shell Elements and Beam Elements

(2nd Report, Strength Evaluation Method)*

Tomohiro NARUSE**, Takeshi KAWASAKI*** and Toshio HATTORI****

**Hitachi, Ltd. Mechanical Engineering Research Laboratory,
832-2, Horiguchi, Hitachinaka, Ibaraki, 312-0034, Japan
E-mail: tomohiro.naruse.az@hitachi.com

***Hitachi, Ltd. Industrial System, Transportation System Division, Kasado Transportation Systems Product Division,
794, Higashitoyoi, Kudamatsu City, Yamaguchi, 744-8601, Japan
E-mail: takeshi.kawasaki.xz@hitachi.com

****Gifu University, Department of Mechanical and Systems Engineering, Faculty of Engineering,
Yanagido 1-1, Gifu City, Gifu, 501-1193, Japan
E-mail: hattori@cc.gifu-u.ac.jp

Abstract

The stiffness of an engineering structure with joints depends not only on the materials and dimensions of the structure but also on the stiffness of the fasteners that connect its components. To evaluate the mechanical behaviour of a complex structure with bolted joints, we first developed a simple finite element (FE) modelling technique that was simplified by using shell and beam elements and accounts for the effect of the stiffness of jointed plates and bolts. In evaluating the mechanical behaviour, we also need a method for evaluating the strength of bolt joints from the results of FE analysis. In this study, we have developed a strength evaluation method for the beam forces of FE analysis by considering the mechanics of bolt joints. This method can be used to evaluate static failure and fatigue failure of bolts and slip on clamped plates and bearing surfaces. We can easily evaluate the strength of bolt joints of industrial products with many bolted joints by using this method.

Key words: Bolted Joint, Finite Element Method, Stress Analysis

1. Introduction

Strength design guidelines of bolted joints had previously evaluated static collapse, fatigue failure, and slip between fastened plates by using stress calculation methods based on material mechanics [(1)~(4)]. However, it is difficult to directly apply these design guidelines to the structures of industrial products having many bolted joints, first because they require load condition of each joint and second because the load prediction method is not sufficiently accurate.

On the other hand, great progress has recently been made in Computer Aided Engineering, or CAE, and this progress has made this technique a practical way to evaluate bolted-joints strength by using finite element (FE) analysis. Papers have been published that precisely calculated the stress and force of bolted joints based on contact analysis of joint

*Received 4 Nov., 2008 (No. T1-06-1160)
Japanese Original : Trans. Jpn. Soc. Mech. Eng., Vol.73, No.728, A (2007), pp.529-536 (Received 22 Nov., 2006)
[DOI: 10.1299/jcst.3.34]

elements [5] and analyzed the loosening phenomenon of bolted joints by taking more complex contact conditions into account [6]. However, if an entire-structure FE model were to be made while taking contact conditions that had previously been reported into consideration, the number of elements would be too large. What is needed, therefore, is a simplified bolted-joints analysis model to enable industrial products structures to be accurately analyzed.

A simple bolted-joint analysis model has been proposed that connects two bolt holes with rigid bar elements [7]. Other simple models with equivalent springs and beams have been proposed to achieve greater accuracy [8]~[11]. In the former, however, bolted-joints stiffness is not considered. In the latter, deformation can be calculated with high accuracy, however, it is not clear as to which strength evaluation method for the model can be applied. What is needed, therefore, is to develop a simple and accurate bolted-joint model that can be applied to any structure with many bolted joints, as well as a strength evaluation method that can be integrated into the model.

In the first paper we published regarding this study, we reported that we had developed a modelling technique that simplifies the bolted-joint structures by using shell and beam elements [12]. This technique took the bolted-joints mechanism into consideration, and is highly accurate despite its simplicity.

In this paper, we propose a strength evaluation method for our simplified bolted-joint model that takes strength design guidelines [1]~[4] into account. This method can be applied to simplified bolted-joint models, for which no clear-cut strength evaluation method had previously been developed.

2. Bolted-Joint Strength Evaluation Method

2. 1 Modelling method of bolted joints

Figure 1 shows the bolted-joint modelling method that we presented in our first paper [12]. This modelling method uses the equivalent beam element, the stiffness of which is determined as comprising the stiffness of the bolt and that of the pressure cone, and the equivalent pressure area, which is defined as being within the pressure cone of two plates. Figure 2 shows a schematic depiction of a bolted joint. In the case when two plates are joined with sufficient clamping force and the contact conditions between the plates are maintained under external force, the subjected external load is transmitted from one plate to the other through the pressure cone shown in the figure. We calculated the axial, bending, and torsional stiffness of the equivalent beam element of a bolted joint as described below.

According to VDI2230 (1977) [4], the axial compliance of a bolt δ_b, which represents the axial stiffness of a bolt, is calculated as

$$\delta_b = \frac{0.4d}{E_b A_n} + \frac{l_g}{E_b A_n} + \frac{l_s}{E_b A_3} + \frac{0.4d}{E_b A_n}, \tag{1}$$

in which d is the nominal diameter of the bolt, E_b is Young's modulus of the bolts, l_g is the length of the cylindrical body as shown in Fig. 2, l_s is the length of the free-loaded thread as shown in Fig. 2, A_n is the nominal cross section, and A_3 is the cross section with a bolt thread diameter of d_3, respectively. According to VDI2230 (1977) [4], pressure cone stiffness is obtained in terms of a tube with an outer diameter equal to the equivalent diameter D_{eq} and an inner diameter equal to the hole diameter D_i, as shown in Fig. 3. The equivalent diameter of the pressure cone D_{eq} and the equivalent cross-section of the pressure cone A_{eq} are expressed by Eqs. (2) and (3). The axial compliance of the pressure cone δ_c is calculated as in Eq. (4).

$$D_{eq} = d_w + \frac{l_f}{10} \quad \left(\text{when } 3d_w < D_c \text{ and } l_f \le 8d\right), \tag{2}$$

$$A_{eq} = \frac{\pi}{4}\left(D_{eq}^2 - D_i^2\right), \tag{3}$$

$$\delta_c = \frac{l_f}{E_c A_{eq}}, \tag{4}$$

in which E_c is Young's modulus of the plates. The load factor Φ is defined by using the δ_b of Eq. (1) and δ_c of Eq. (4) as in the following equation:

$$\Phi = \frac{\delta_c}{\delta_b + \delta_c}. \tag{5}$$

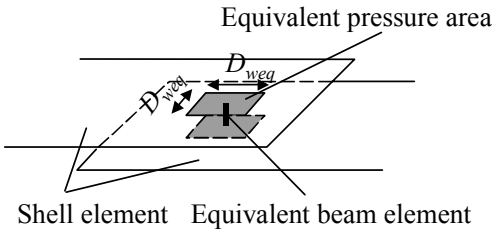

Fig. 1 Equivalent model of bolted joints

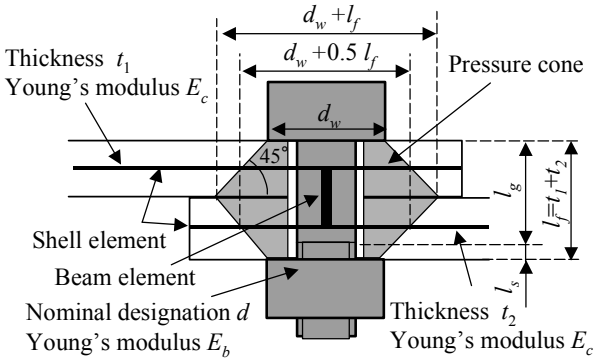

Fig. 2 Structure and model of bolted joints

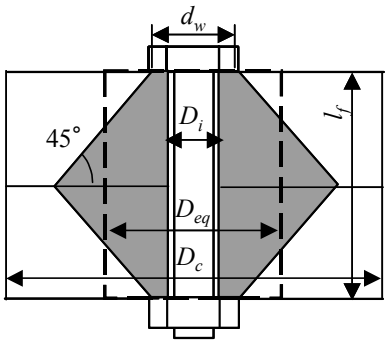

Fig. 3 Equivalent diameter of pressure cone

If Young's modulus of the equivalent beam is E_b, the cross section of equivalent beam A_{beq} and the equivalent diameter for the axial load d_{eq1} are obtained from Eq. (6):

$$A_{beq} = \frac{\pi}{4} d_{eq1}^2 = \frac{l_f}{E_b \delta_b \Phi}. \tag{6}$$

The bending compliance of the bolt β_b is a serial connection of cylinders similar to that shown in Eq. (1).

$$\beta_b = \frac{0.4d}{E_b I_n} + \frac{l_g}{E_b I_n} + \frac{l_s}{E_b I_3} + \frac{0.4d}{E_b I_n} \tag{7}$$

Here, I_n is the second moment of the nominal cross section, and I_3 is the second moment of the bolt thread section. The bending stiffness of the pressure cone is also assumed to be a tube with an outer diameter equal to the equivalent diameter D_{eq} and an inner diameter equal to the hole diameter D_i, as shown in Eq. (8).

$$\beta_c = \frac{l_f}{E_c I_{eq}} = \frac{64 l_f}{\pi E_b \left(D_{eq}^4 - D_i^4\right)} \tag{8}$$

The load factor for the bending moment, Φ_b, is defined as in the following equation:

$$\Phi_b = \frac{\beta_c}{\beta_b + \beta_c}. \tag{9}$$

We obtain the second moment of the equivalent beam I_{beq} and the equivalent diameter for the bending stiffness d_{eq2} from Eq. (10):

$$I_{beq} = \frac{\pi}{64} d_{eq2}^4 = \frac{l_f}{E_b \beta_b \Phi_b}. \tag{10}$$

We considered the torsional stiffness of an equivalent beam to be similar to the bending stiffness. The polar second moment of the equivalent beam element is equal to twice the second moment of the equivalent beam element I_{beq}. The load factor for the torque, therefore, is identical to the load factor for the bending moment Φ_b.

We set the equivalent pressure area to a square with a length of $D_{weq}=d_w+0.5l_f$, and the shell element nodes within the equivalent pressure area are constrained to the tip node of the equivalent beam node. These boundary conditions are represented by the constraint equations, in which the tip node of the equivalent beam is the master node and the shell element nodes within the equivalent pressure area are slave nodes. These constraint equations can be simply defined by using the CERIG command in ANSYS®.

2. 2 Working loads of bolted joints

Bolted joints should be designed to maintain preloads at assembly and working loads. Working loads on each bolted joint had been calculated by dividing total working loads by the bolt number or had been estimated from the geometric equilibrium of force in strength evaluation guidelines [(1)~(3)]. These estimated working loads on each bolted joint therefore contained many errors. On the other hand, the modelling method of bolted joints that we described in our previous paper can easily calculate the working loads on each bolted joint as the output forces of the beam element. Since these output forces obtained with the model that takes the stiffness of bolted joints into consideration, they are more accurate than the working loads estimated by using strength evaluation guidelines.

Figure 4 shows a schematic depiction of output forces and moments of a beam element. The output forces are calculated on the coordinate system of the beam element. We can estimate the axial force W_a, shear force W_s, bending moment M, and torque T of the working loads from these output forces and moments as follows:

$$W_a = F_x, \tag{11}$$

$$W_s = \sqrt{F_y^2 + F_z^2}, \tag{12}$$

$$M = \max\left(\sqrt{M_{yi}^2 + M_{zi}^2}, \sqrt{M_{yj}^2 + M_{zj}^2}\right), \tag{13}$$

$$T = \left|M_x\right|. \tag{14}$$

Evaluating the bolted-joints strength mainly comprises evaluating [1] static strength, [2] fatigue strength and [3] slip. In addition to these primary evaluations, we evaluate [4] the pressure on the bearing surfaces and the preload change caused by embedding of the contact

surface and thermal deformation. These four evaluations are explained in the following sections.

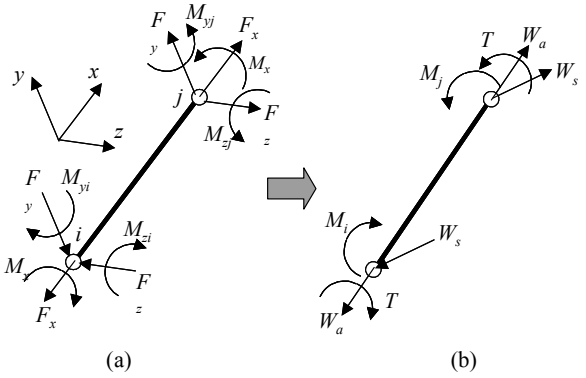

(a) (b)

Fig. 4 Forces and moments of equivalent beam element of bolt

2. 3 Static strength evaluation

When a bolt with a nominal diameter d is tightened with a torque T_f, the pretension F_f is calculated as in Eq. (15).

$$F_x = \frac{T_f}{Kd} \tag{15}$$

Here, K is called the "nut factor", which from Eq. (16) is calculated with the friction coefficient between nut and bolt threads, μ_s, the friction coefficient in the head bearing area, μ_w and the thread dimensions.

$$K = \frac{1}{2d}\left(\frac{P}{\pi} + \mu_s d_2 \sec\alpha' + \mu_w D_w\right) \tag{16}$$

Here, P is the thread pitch, d_2 is the effective diameter of the thread, α' is calculated as $\tan\alpha' = \tan\alpha + \tan\beta$ from the half-angle of the threads α and the lead angle of the threads β, and D_w is called the effective diameter of the head bearing surface, and it is obtained as following equation from the outer diameter of bearing area D_o and the hole diameter D_i:

$$D_w = \frac{2}{3}\frac{D_o^3 - D_i^3}{D_o^2 - D_i^2}. \tag{17}$$

Since the friction coefficients vary widely and are hard to predict, the pretension scatter should be taken into consideration when bolts are tightened with the torque control method. If the scatter of the pretension is m%, the maximum pretension $F_{f\max}$ and the minimum pretension $F_{f\min}$ are expressed with F_f of Eq. (15) as follows:

$$F_{f\max} = (1 + m/100)F_f, \tag{18}$$

$$F_{f\min} = (1 - m/100)F_f. \tag{19}$$

The scatter m is considered to be 15% in general.

From the above pretension values and the working forces as described in Section 2.2, the bolt stresses can be estimated. The stress on the thread section is calculated from the effective thread section A_s. The diameter of the effective thread section, d_s, is the average of the pitch diameter of the bolt thread, d_2, and the minor diameter of the bolt thread, d_3, i.e.:

$$d_s = \frac{d_2 + d_3}{2}. \tag{20}$$

In static strength evaluation, the maximum pretension $F_{f\max}$ shown in Eq. (18) is used. The maximum axial stress $\sigma_{f\max}$ on the effective thread section A_s under the pretension is obtained by:

$$\sigma_{f\max} = \frac{F_{f\max}}{A_s}. \tag{21}$$

The maximum shear stress $\tau_{f\max}$ on the thread under the pretension is calculated by dividing the maximum torque $T_{s\max}$ under the pretension by the torsional section modulus Z_{ps} with the diameter of the effective thread section expressed as in the following equation.

$$\tau_{f\max} = \frac{T_{s\max}}{Z_{ps}} = \frac{8F_{f\max}d_2}{\pi d_s^3}\left(\tan\beta + \frac{\mu_s}{\cos\alpha'}\right) \tag{22}$$

To prevent the bolt from yielding under the pretension, the equivalent stress of the thread σ_{e1}, which is calculated from $\sigma_{f\max}$ of Eq. (21) and $\tau_{f\max}$ of Eq. (22), should be smaller than the yield strength σ_{by} of the bolt material, taking the safety factor a_y into consideration, i.e.:

$$\sigma_{e1} = \sqrt{\sigma_{f\max}^2 + 3\tau_{f\max}^2} < \sigma_{by}/a_y. \tag{23}$$

Next, we consider how to evaluate the static strength under the working forces W_a, W_s, M, and T shown in Fig. 4(b). As previously mentioned, a bolted joint supports the working forces by dividing the forces between those of the bolt and those of the plates. In this case, the stresses caused by the shear force W_s and the bending moment M are so small that static failure caused by these working forces and moments do not need to be considered.

What needs to be evaluated, therefore, is the static strength by adding the stresses caused by the axial working force W_a and the working torque T to the stress under the pretension. When the bolt joint is subjected to the axial working force W_a, the bolt sustains the divided force ΦW_a and the plates support the force $(1-\Phi)W_a$. Here, Φ is the load factor defined by Eq. (5). The stress σ_n on the effective thread section under the axial working force W_a is obtained by the following equation:

$$\sigma_n = \frac{\Phi W_a}{A_s}. \tag{24}$$

Here, when the bolted joint is subjected to the working torque T, the bolt and the plates sustain the working torque together. The load factor of the torque is identical to the load factor of the bending moment, Φ_b. Thus, the shear stress τ_s on the effective thread section under the working torque, T, is calculated as

$$\tau_s = \frac{\Phi_b T}{Z_{ps}}. \tag{25}$$

To prevent the bolt from yielding under the working forces, the equivalent stress of the thread σ_{e2}, which is calculated from $\sigma_{f\max}$ of Eq. (21), $\tau_{f\max}$ of Eq. (22), σ_n of Eq. (24), and τ_s of Eq. (25) should be smaller than the yield strength of the bolt material σ_{by}, taking the safety factor a_y into consideration, i.e.:

$$\sigma_{e2} = \sqrt{(\sigma_{f\max} + \sigma_n)^2 + 3(\tau_{f\max} + \tau_s)^2} < \sigma_{by}/a_y. \tag{26}$$

From the above static strength evaluation, we can determine the nominal diameter of the bolt by satisfying Eq. (23) and Eq. (26) under the pretension and the working forces, respectively.

2. 4 Fatigue strength evaluation

Fatigue failure in a thread is caused by the cyclic stress on the axial direction under the working forces. From the stresses under the working forces W_a, W_s, M, and T shown in Fig. 4 (b), we take the axial stress σ'_n under the axial force W_a and the bending stress σ'_b under the bending moment M into consideration. The axial stress σ'_n and the bending stress σ'_b, are calculated on the cross section of the minor diameter d_3. The axial stress σ'_n under the axial force W_a is calculated by using the load factor Φ defined by Eq. (5) as:

$$\sigma'_n = \frac{\Phi W_a}{A_3}, \tag{27}$$

in which A_3 is the cross section of the minor diameter, d_3.

The bending stress σ'_b under the bending moment M is calculated by using the load factor Φ_b defined by Eq. (9) as:

$$\sigma'_b = \frac{\Phi_b M}{Z_3}, \tag{28}$$

in which Z_3 is the section modulus of the minor diameter, d_3.

Yamamoto et al. [1] found that the tread fatigue strength is almost constant when the pretension is sufficient. They also estimated the thread fatigue strength σ_{wk} by taking the stress concentration of the thread, the fatigue notch factor, and the fatigue strength of the bolt material into account. This estimated fatigue strength σ_{wk} is calculated with ISO strength classes and the nominal diameters [1]. To prevent the bolt from incurring fatigue failure, the thread stress amplitude σ_a, which is calculated from σ'_n of Eq. (27) and σ'_b of Eq. (28), should be smaller than this estimated fatigue strength σ_{wk} while taking the safety factor a_w into consideration.

$$\sigma_a = \max\left(\frac{\left|\sigma'_n + \sigma'_b\right|}{2}, \frac{\left|\sigma'_n - \sigma'_b\right|}{2}\right) < \frac{\sigma_{wk}}{a_w} \tag{29}$$

2. 5 Slip evaluation

When a bolted joint is subjected to working forces, it should be designed not to slip on the bearing surface between the bolt head and the plate, or between the nut and the plate, or on the surface between the two plates. The static friction forces on the bearing surfaces and on the surface between two plates, therefore, should be larger than the working forces. The static friction forces are calculated by multiplying the friction coefficients by the normal forces on these surfaces. The friction coefficient on the bearing surface is μ_w, and that on the surface between the two plates is μ_c. In the slip evaluation, the nominal forces on these surfaces are estimated by adding the axial additional bolt load by the axial force W_a and the minimum pretension $F_{f\min}$ defined by Eq. (19).

The nominal force on the bearing surface is increased by ΦW_a from the minimum pretension $F_{f\min}$ under the axial force W_a. Here, Φ is the load factor defined by Eq. (5). The static friction force F_w is calculated as

$$F_w = \mu_w\left(F_{f\min} + \Phi W_a\right). \tag{30}$$

The nominal force on the surface between the two plates is decreased by $(1-\Phi)W_a$ from the minimum pretension $F_{f\min}$ under the axial force W_a. The static friction force F_c is calculated as:

$$F_c = \mu_c\left\{F_{f\min} - (1-\Phi)W_a\right\}. \tag{31}$$

We compared these static friction forces with the shear force W_s and torque T. To prevent the bolt joint from slipping under the shear force W_s, the following inequalities should be satisfied while taking the safety factor a_s into consideration:

$$W_s < F_w / a_s, \tag{32}$$

$$W_s < F_c / a_s. \tag{33}$$

Further, to prevent the bolt joint from slipping on the bearing surface under torque T, the following inequality should be satisfied while taking the safety factor a_s into consideration:

$$T < \frac{F_w}{a_s} \times \frac{D_w}{2}. \tag{34}$$

Here, D_w is the effective radius of the head bearing surface defined by Eq. (17). The

pressure cone diameter is so large that the surface between the two plates might not slip under torque T. Therefore, only the slippage on the bearing surface should be evaluated under torque T.

2. 6 Evaluating pressure on bearing surfaces and the preload changes caused by embedding and thermal deformation

In this section, we evaluate the pressure on the bearing surfaces and preload changes caused by embedding on the contact surface and thermal deformation. Bearing surface pressure causes yield and creep deformation on the contact surfaces, and it loosens the bolted joints. The limit pressure on the bearing surface has been obtained for various materials of plates experimentally in some literature [(1)~(4)]. We compared the bearing surface pressures under the preload and under working forces to this limit pressure of the plates' materials, p_L.

$$\frac{F_{f\max}}{A_w} < p_L, \quad \frac{F_{f\max} + \Phi W_a}{A_w} < p_L \tag{35}$$

Here, A_w is the bearing surface area, which is calculated with the outer diameter of the bearing surface D_o and the hole diameter D_i.

$$A_w = \frac{\pi}{4}\left(D_o^2 - D_i^2\right) \tag{36}$$

Next, we evaluate the preload change caused by embedding on the contact surface. Embedding on the contact surface occurs when microscopic roughness on the contact surface is smoothened by yield deformation and it results decreasing the preload. The preload loss F_{z1} resulting from embedding is calculated from the permanent deformation on the bearing surface f_z, the load factor Φ defined by Eq. (5), and the compliance of the plates δ_c defined by Eq. (4) as:

$$F_{z1} = \frac{\Phi}{\delta_c} f_z . \tag{37}$$

Several methods for calculating the permanent deformation f_z on the bearing surface have been proposed in conjunction with experimental results [(1)~(4)]. Here, VDI2230 equation [(4)] is shown as Eq. (38), which is obtained from the nominal diameter d and the clamping length l_f. Since this equation (38) is calculated in terms of micrometer, the micrometer unit needs to be changed to the unit of Eq. (37), when Eq. (38) is substituted into Eq. (37).

$$f_z = 3.29\left(\frac{l_f}{d}\right)^{0.34} \quad (\mu m) \tag{38}$$

We evaluated the pretension change incurred by embedding on the contact surface while substituting the minimum pretension term $F_{f\min}$ described in Section 2.5 into ($F_{f\min}$ - F_{z1}).

Next, we considered the preload change caused by thermal deformation. When the thermal expansion coefficients are different between the bolt material and the plate materials, and the bolted joint temperatures are varied, the preload would change with thermal deformation. The modelling method of bolted joints by using shell and beam elements described in Section 2.1 can estimate the in-plane deformation by thermal expansion. However, shell elements cannot evaluate the thermal deformation in the thickness direction. Thus, the preload change cased by the thermal deformation in the thickness direction should be evaluated by the following method:

The thermal expansion coefficients of the bolt and the plates are determined as α_b and α_c respectively. The temperature rises in the bolt and the plates are represented by Δt_b and Δt_c respectively. The preload loss F_{z2} determined by the thermal deformation result is calculated from the load factor Φ defined by Eq. (5), the compliance of the plates δ_c defined by Eq. (4) and the clamping length l_f as:

$$F_{z2} = \frac{\Phi}{\delta_c}\left(\alpha_b \Delta t_b - \alpha_c \Delta t_c\right) l_f \,. \tag{39}$$

We can evaluate the pretension change resulting from the thermal deformation by substituting the term of the axial force change ΦW_a in Sections 2.3, 2.4 and 2.5 and the pressure evaluation on the bearing surface described in Section 2.6 into (ΦW_a - F_{z2}).

3. Application of the Developed Strength Evaluation Method

3. 1 Analysis model

We applied our strength evaluation method to the specific example shown in Fig. 5, which we also analyzed in our first paper [12]. Three channels were assembled into an H-shaped structure and tightened down with four M12 bolts at each of two intersections. The structure was fixed in place at the four ends and subjected to an out-of-plane load at the centre. Taking the symmetry into consideration, the analysis model was a half model as shown in Fig. 6. The analysis was carried out with ANSYS® 7.1. We made an FE model by using our modelling method for bolted joints described in Section 2.1. The x-axis of the coordinate system corresponded to the axial directions of bolts.

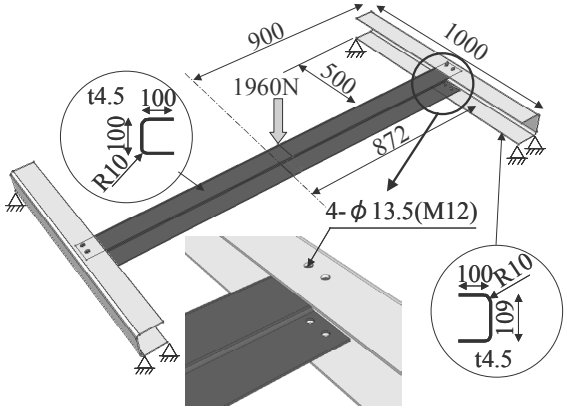

Fig. 5 Example of bolted joint structure

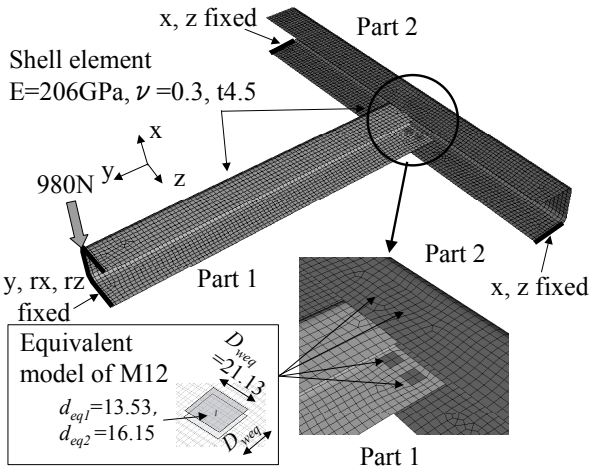

Fig. 6 Analysis model of example

3. 2 Strength evaluation

Figure 7 shows the results obtained for the working forces F_x and F_y loaded to four equivalent beam elements of bolted joints 1-4. Working force F_z and moments M_x, M_y and M_z were obtained as well. These forces and moments are shown in Table 1. Taking the force directions into consideration, axial force W_a, shear force W_s, bending moment M, and torque T calculated by using Eq. (11)~(14) are also shown in Table 1.

As an example of strength evaluation, we evaluated bolt no. 1 under the forces shown in Table 1. Table 2 shows inputs with ISO class 4.8 and 8.8 bolts and with SS400 carbon steel plates, the results indicating evaluated static strength, fatigue strength, slip, bearing surface pressure, and preload change.

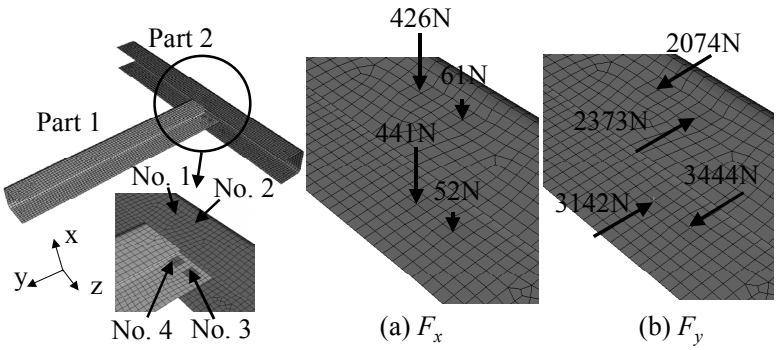

Fig. 7 Load distribution of analysis results

Table 1 Load distribution of bolts

No. of bolt	No. 1	No. 2	No. 3	No. 4
F_x [N]	-426	-61	-52	-441
F_y [N]	2074	-2377	3444	-3142
F_z [N]	-159	21	29	109
M_x [N·mm]	13131	9565	-15411	-17649
M_y [N·mm]	-4579	1974	2159	-4662
M_z [N·mm]	-12257	9533	12129	-14938
W_a [N]	426	61	-52	-441
W_s [N]	2080	2377	3444	3144
T [N·mm]	13131	9565	15411	17649
M [N·mm]	13084	9735	12320	15649

We determined the pretension as being 70% of the yield tightening torque T_{fy} with the friction coefficient μ_w=0.15 on the bearing surface written in JIS 1083. The friction coefficient μ_s on the thread surface is equal to the friction coefficient μ_w of 0.15 on the bearing surface. The nut factor is K=0.199 according to JIS 1083. We calculated the pretension F_f from Eq. (15), and obtained the maximum and minimum pretensions with scatter m of 15% obtained by Eqs. (18) and (19). We estimated the preload loss obtained by embedding on the contact surface from Eqs. (37) and (38). We also estimated safety factors of static strength, fatigue strength, slip, and bearing surface pressure as ratios of the allowable and the calculated value.

If the bolt is an ISO class 4.8 bolt, the slip evaluation safety factor is smaller than 1.0 as shown in the grey cell in Table 2. This shows that the bolted joint cannot hold the shear force W_s and would slip between the two plates. If the bolt is an ISO class 8.8 bolt, the bolted joints could be tightened with higher pretension and the static friction force would be increased. The slip evaluation safety factor, therefore, would increase to greater than 1.0.

On the other hand, when the bolt is an ISO class 8.8 bolt, the safety factor of the bearing surface pressure is smaller than 1.0 as shown in the grey cell in Table 2. The bearing surface pressure is so high that the bearing surfaces on the two plates are significantly deformed plastically. Thus, the plate materials need to be changed to those having higher yield strength. Alternatively, wide-diameter washers need to be used to decrease the bearing surface pressure.

We also evaluated fatigue strength by calculating the stress amplitude from the axial

force W_a and the bending moment M as shown in Table 2. Preload changes caused by thermal deformation can be evaluated in this way, however we found that in this model such changes need not be evaluated because the bolt and plate materials are carbon steel types.

Table 2 Example of strength evaluation of No. 1 bolt

		Parameter name	Symbol	Dimension	Input and output	
Input		Nominal designation	d	[mm]	12	
		Thread pitch diameter	d_2	[mm]	10.863	
		Thread root diameter	d_3	[mm]	10.106	
		Hole diameter	D_i	[mm]	13.5	
		Outer bearing diameter	d_w	[mm]	16.63	
		Young's modulus of bolt	E_b	[GPa]	206	
		ISO grade			4.8	8.8
		Yield strength of bolt material	σ_{by}	[MPa]	340	640
		Fatigue strength of bolt	σ_{wk}	[MPa]	48	53
		Tightening torque	T_f	[N·mm]	38000	69000
		Pretension	F_f	[N]	16150	29325
		Maximum pretension	F_{fmax}	[N]	18573	33724
		Minimum pretension	F_{fmin}	[N]	13728	24927
		Young's modulus of plate	E_c	[GPa]	206	
		Thickness of plate 1	t_1	[mm]	4.5	
		Thickness of plate 2	t_2	[mm]	4.5	
		Friction coefficient of bearing surface	μ_w		0.15	
		Friction coefficient of clamped plate	μ_c		0.15	
Output	Stiffness calculation	Compliance of bolt	δ_b	[mm/N]	9.567E-07	
		Compliance of clamped plates	δ_c	[mm/N]	4.448E-07	
		Load factor	Φ		0.3174	
		Bending compliance of bolt	β_b	[1/N·mm]	1.311E-07	
		Bending compliance of clamped plate	β_c	[1/N·mm]	1.454E-08	
		Load factor for bending moment	Φ_b		0.0998	
	Preload loss	Permanent deformation of bearing surface	f_z	[μm]	2.9830	
		Pretension loss	F_{z1}	[N]	2129	
	Stress calculation	Axial stress due to pretension	σ_{fmax}	[MPa]	215	391
		Shear stress due to pretension	τ_{fmax}	[MPa]	100	182
		Axial stress due to axial load W_a	σ_n	[MPa]	1.6	
		Shear stress due to torque T	τ_s	[MPa]	66.7	
		Axial stress at thread root area due to axial load W_a	σ'_n	[MPa]	1.7	
		Axial stress at thread root area due to bending moment M	σ'_b	[MPa]	12.9	
		Equivalent stress due to pretension	σ_{e1}	[MPa]	276	502
		Equivalent stress due to pretension and working loads	σ_{e2}	[MPa]	284	509
		Stress amplitude	σ_a	[MPa]	7.3	
	Evaluation for stress	Safety factor for equivalent stress due to pretension	σ_{by}/σ_{e1}		1.23	1.28
		Safety factor for equivalent stress due to pretension and working loads	σ_{by}/σ_{e2}		1.20	1.26
		Safety factor for fatigue strength	σ_{wk}/σ_a		6.59	7.27
	Evaluation for slip	Static frictional force on bearing surface	F_w	[N]	1760	3440
		Static frictional force on clamped plate	F_c	[N]	1696	3376
		Safety factor for slip on bearing surface by shear force W_s	F_w/W_s		**0.85**	1.65
		Safety factor for slip on clamped plate by shear force W_s	F_c/W_s		**0.82**	1.62
		Safety factor for slip on bearing surface by torque T	$F_w D_w/2/T$		1.01	1.98
	Evaluation for bearing surface pressure	Pressure due to pretension	F_{fmax}/A_w	[MPa]	251	455
		Pressure due to pretension and working loads	$(F_{fmax}+\Phi W_a)/A_w$	[MPa]	224	428
		Allowable pressure (for low carbon steel, SS400)	p_L	[MPa]	260	
		Safety factor for pressure due to pretension	$p_L A_w/F_{fmax}$		1.04	**0.57**
		Safety factor for pressure due to pretension and working loads	$p_L A_w/(F_{fmax}+\Phi Wa)$		1.16	**0.61**

4. Conclusion

We aimed to develop a strength evaluation method of bolted joint for the FE model that we described in our first paper [12] that simplifies the bolted-joint structures by using shell and beam elements. We obtained the following results in our work:

1) We proposed a reliability evaluation method for the bolted joints in the FE model that estimate the static and fatigue strength of bolt and their slip limit by calculating the forces and moments of equivalent beam and considering the mechanism of the bolted joints.
2) We applied our strength evaluation method to a specific example having many bolted joints and found that it was able to evaluate the bolt reliability.

Our method does not take the contact condition of bolted joints into consideration and, thus, it is unable to evaluate opening and slippage on the contact surface. However, when a structure many bolted joints is considered, our method provides sufficient information in most cases, while conventional modelling methods do not have a definite method of the strength evaluation.

References

(1) Yamamoto, A., *Theory and Design of Bolt Joints* (in Japanese), (1977), pp. 30-69, Yokendo
(2) Yoshimoto, I., *Points for Design of Bolt Joints* (in Japanese), (1992), pp. 177-215, Japanese Standards Association
(3) Editorial board of handbook of joint technique, *Handbook of Joint Technique* (in Japanese), (1994), pp. 615-640, Industrial service centre
(4) VDI-Richtline 2230 (1977)
(5) Fukuoka, T., *Finite Element Simulation of Mechanical Behaviors and Seal Performance of Oil Seal Plug*, Transactions of the Japan Society of Mechanical Engineers, Series A, Vol. 64, No. 625 (1998), pp. 2395-2401
(6) Izumi, S. et al., *Three-dimensional Finite Element Analysis of Tightening and Loosening Mechanism of Bolted Joint*, Transactions of the Japan Society of Mechanical Engineers, Series A, Vol. 71 No. 702 (2005), pp. 204-212
(7) ANSYS, ICEM CFD/AI*Environment 5.1 Introductory User Course (FEA)
(8) Kim, J.G. et al., *Finite Element Modelling and Experimental Verification of the Structures with Bolted Joints*, Transactions of the Korea Society of Mechanical Engineers, 20–6(1996), pp. 1854-1861
(9) Hurrell, P. R., *Good Practice in Modelling of Pressure Vessel Bolted Joints for Stress and Fatigue Analysis*, ASME Pressure Vessels & Piping Conference, Vol. 405(2000), pp. 123-134
(10) Montgomery, J., *Methods for Modeling Bolts in the Bolted Joint*, ANSYS 2002 Conference, 2002 April,
(11) Rutman, A. and Kogan, J. B., *Software takes the load off joint modeling*, Machine Design, Vol. 70, No. 6 (1998), pp. 79-82
(12) Naruse, T. et al., *Simple Modelling and Strength Evaluation Methods for Bolt Joints Using Shell Elements and Beam Elements ((1) Modelling Method)*, Transactions of the Japan Society of Mechanical Engineers, Series A, Vol. 73, No. 728 (2007), pp. 522-528